



Ultraviolet absorption cross-sections of hot carbon dioxide

Matthew A. Oehlschlaeger^{*}, David F. Davidson, Jay B. Jeffries, Ronald K. Hanson

High Temperature Gasdynamics Laboratory, Department of Mechanical Engineering, Stanford University, Stanford, CA 94305-3032, USA

Received 7 September 2004; in final form 11 October 2004

Available online 2 November 2004

Abstract

The temperature-dependent ultraviolet absorption cross-section for CO₂ has been measured in shock-heated gases between 1500 and 4500 K at 216.5, 244, 266, and 306 nm. Continuous-wave lasers provide the spectral brightness to enable precise time-resolved measurements with the microsecond time-response needed to monitor thermal decomposition of CO₂ at temperatures above 3000 K. The photophysics of the highly temperature dependent cross-section is discussed. The new data allows the extension of CO₂ absorption-based temperature sensing methods to higher temperatures, such as those found in behind detonation waves.

© 2004 Elsevier B.V. All rights reserved.

1. Introduction

Accurate ultraviolet (UV) absorption cross-sections for CO₂ at high-temperatures are needed for many applications including: combustion and flow diagnostics, photolytic conversion of CO₂ to CO, and the modeling of planetary atmospheres. Many previous studies [1] have focused on the absorption in the vacuum UV by room temperature CO₂ but few have investigated the absorption at elevated temperature or for wavelengths longer than 200 nm. At longer UV wavelengths absorption by hot CO₂ occurs primarily due to pre-dissociative transitions in the CO₂(¹B₂) ← CO₂(¹Σ_g⁺) electronic system [2,3]. However, small contributions to the cross-section may also come from transitions to the ¹A₂, ³A₂, and ³B₂ states [4,5]. Here we present new absorption cross-section measurements made behind reflected shock waves at high temperatures (1500–4500 K) utilizing time-resolved absorption of four selected continuous-wave (cw) lasers at 216.5, 244, 266, and 306 nm. Recently, Schulz et al. [6] have shown that the UV CO₂ absorption feature is spectrally

smooth at wavelengths longer than 190 nm. The continuous nature of the absorption and its strong wavelength- and temperature-dependence allow for temperature sensing strategies using two laser wavelengths as demonstrated by Jeffries et al. [7]. This study extends the absorption cross-section measurements of Schulz et al. [6] to the higher temperatures needed to study the gas temperature behind detonation waves.

Previous studies of the CO₂ absorption cross-section at high temperatures in the range from 190 to 355 nm have utilized shock tubes [2,6,8,9], furnaces [3,10], and laminar flames [11]. The earliest of these studies, carried out by Generalov et al. [8], reported the cross-section at 238 and 300 nm measured behind shock waves at temperatures of 1400–6300 K, but their cross-section results are uncertain because of difficulty in correcting for time-dependent CO₂ dissociation with the instrumentation of the era. Ibreighith and Roth [9] reported cross-section measurements at 214.7 and 236 nm made behind shock waves at temperatures of 1400–2800 K and Koshi et al. [2] have reported cross-sections at 193 nm measured behind shock waves at temperatures of 1500–2700 K. Hartinger et al. [10] have measured cross-sections at 193 nm in an electrically heated furnace at 573–1273 K and Jensen et al. [3] have published UV cross-sections (230–350 nm) at 1523–2273 K also measured in a

^{*} Corresponding author. Fax: +1 650 723 1748.

E-mail address: moehlsch@stanford.edu (M.A. Oehlschlaeger).

furnace. Joutsenoja et al. [11] measured the UV absorption cross-section of CO₂ in a laminar pre-mixed flame across the wavelength range of 200–270 nm and temperature range 1400–1700 K. Schulz et al. [6] reported the absorption spectrum of shock-heated CO₂ between 200 and 320 nm from 900 to 3050 K. Most recently laser-induced fluorescence from CO₂ was observed following UV absorption [12,13].

The strong temperature-dependence of the absorption cross-section has enabled new UV absorption-based temperature measurement strategies in combustion gases [7,14]. A CO₂ thermometry diagnostic [7,14] requires precise absorption data over an extended temperature range and this need motivates this work. Additionally, the temperature-dependence of the absorption cross-section measurements enables us to speculate on the photophysics of CO₂ UV absorption.

This work follows up on previous CO₂ absorption cross-section measurements made in our laboratory [6] in which light from a deuterium lamp was transmitted through shock-heated gas mixtures and dispersed with a small imaging monochromator; the time-resolved transmission spectrum (10 μs time resolution) was recorded with a modified frame transfer CCD camera (kinetic spectrograph). These measurements provided the UV CO₂ absorption spectrum from 900 to 3050 K, found that this absorption feature is spectrally smooth, and suggested use of the strong wavelength- and temperature-dependence of the feature for high-temperature sensing strategies. However, the limited spectral brightness of the deuterium lamp limited the signal-to-noise ratio and required millisecond temporal averaging. Because of this time averaging, the previous work above 2300 K required corrections for thermal decomposition of CO₂, and these corrections limited the maximum temperature to 3050 K. The current experiments were performed using light from cw lasers at selected wavelengths detected with UV photodiodes with a wide dynamic range. The increased spectral brightness and detection sensitivity enables microsecond time resolution with a tenfold increase in signal-to-noise. This improved time resolution enables direct monitoring of the thermal decomposition of the CO₂, and thus allows an extension of the temperature range from 3000 to 4500 K. The absorption cross-section at these very high temperatures is of interest for temperature sensing behind detonation waves [14] where many other diagnostic techniques utilizing discrete absorption transitions become difficult because of collisional broadening at the high pressures. In addition, the time-resolution of the experiments enables a determination of the absorption cross-section immediately following the passage of the shock wave, hence, none of the data presented here require chemical model-based corrections for thermal decomposition.

2. Experimental

Mixtures of 2%, 5%, and 10% CO₂ dilute in argon were studied behind reflected shock waves, which provide stationary gas mixtures at known initial temperature and pressure. Experiments were performed in a high-purity pressure-driven stainless steel shock tube (14.13 cm diameter) that has been described elsewhere [15]. The initial pressure and temperature of the post-shock experimental conditions were calculated from the ideal shock wave relations and the measured incident shock speed. The pressure and temperature were taken to be the vibrationally equilibrated conditions. As discussed below, the vibrational relaxation time is very short (~1–5 μs depending on temperature and pressure) behind the reflected shock wave in these experiments. The vibrationally relaxed experimental temperature and pressure have uncertainties of 0.6% and 1.1%, respectively [16]. The gas samples were mixed external to the shock tube in a stainless steel tank with an internal stirring system with research grade gases (99.998% CO₂ and 99.999% Ar). Absorption measurements were made at a location 2 cm from the endwall of the shock tube through UV-grade fused silica windows. The reflected shock conditions ranged from 1500 to 4500 K and 40 to 170 kPa.

CW laser radiation was generated at four different wavelengths: 216.5 nm (2–3 mW) was generated by doubling the output of an Ar⁺ pumped dye-laser, operating at 433 nm, in a BBO external frequency-doubling cavity, previously described in our methyl radical work [15]; 306 nm (2–3 mW) was generated by intra-cavity frequency doubling in a Nd:YVO₄-pumped (532 nm) dye laser operating at 612 nm, as described in our OH radical studies [17]; and 244 and 266 nm (1.5 mW each) were produced by the single pass of a focused laser beam at 488 nm (Ar⁺ line) or 532 nm (Nd:YVO₄) through angle-tuned BBO. The harmonics (244 and 266 nm) were separated from the fundamental beams (488 and 532 nm) with a set of Pellin-Broca prisms.

The UV laser beams were split into two components: one, less than 1 mm in diameter, passing through the shock tube to be absorbed by CO₂(*I*), and one detected prior to absorption as a reference (*I*₀). These two beams were detected using amplified S1722-02 Hamamatsu silicon photodiodes (risetime <1.0 μs, 4.1 mm diameter) and recorded on a digital oscilloscope. The absorption cross-sections were determined using Beer's law

$$I/I_0 = \exp(-\sigma(\lambda, T)nL),$$

where *I* is the transmitted laser intensity, *I*₀ is the reference beam intensity, $\sigma(\lambda, T)$ [cm² molecule⁻¹] is the wavelength- and temperature-dependent CO₂ absorption cross-section, *n* [molecules cm⁻³] is the CO₂ number density, and *L* is the absorption path length (diameter of the shock tube 14.13 cm). For these experiments the

minimum detectable absorbance ($\ln(I_0/I)$) was $<0.1\%$ and absorption cross-sections were not derived for experiments in which the absorbance was less than 0.7% .

The absorbance ($\ln(I_0/I)$) traces for several experiments are shown in Fig. 1. The passage of the incident and reflected shock waves cause two schlieren spikes in the signal, due to steering of the beam off the detector. After the passage of the reflected shock (marked by a strong schlieren induced signal), there is a very short risetime in the absorption signal ($\sim 1\text{--}5\ \mu\text{s}$ depending on the temperature and pressure) prior to the steady absorption due to hot CO_2 . The absorption cross-section is determined during this plateau. This short induction time is caused by the CO_2/Ar V-T relaxation process [18,19] which brings the vibrationally cold CO_2 to an excited vibrational condition where absorption is possible. The observation of this induction time provides evidence that the high-temperature UV absorption of CO_2 comes from a vibrationally excited CO_2 ground state ($^1\Sigma_g^+$). It has been shown by Spielfiedel et al. [20] that molecules with excited bending modes could account for the hot CO_2 absorption at wavelengths longer than $200\ \text{nm}$ because of the significantly better Franck–Condon overlap these states have with the bent $\text{CO}_2(^1B_2)$ electronically excited upper state. The data shown in Fig. 1 are at temperatures below $3000\ \text{K}$ and do not show significant thermal decomposition in the first $200\ \mu\text{s}$.

At higher temperatures ($>3000\ \text{K}$) the CO_2 undergoes thermal decomposition and the absorption traces show temporal decay at long times behind the reflected shock; an example experiment is shown in Fig. 2. This example (Fig. 2) shows a significant induction prior to constant absorption following the incident shock due to vibrational relaxation; the vibrational equilibrated conditions behind the incident shock are $1812\ \text{K}$ and $16.3\ \text{kPa}$. Although, the vibrational relaxation is resolved after

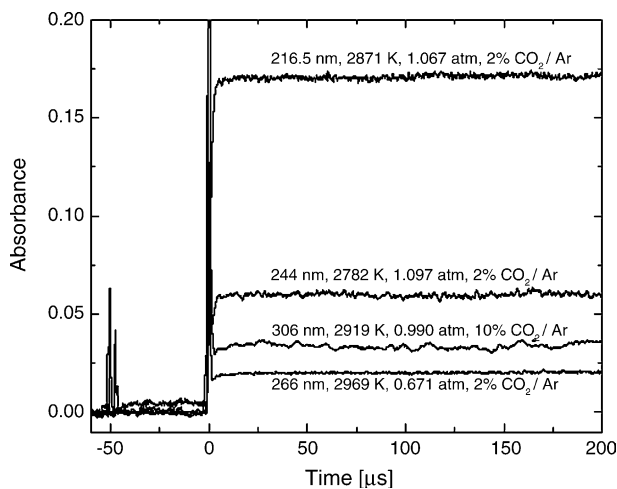


Fig. 1. Example CO_2 absorbance ($\ln(I_0/I)$) for experiments at 216.5, 244, 266, and 306 nm.

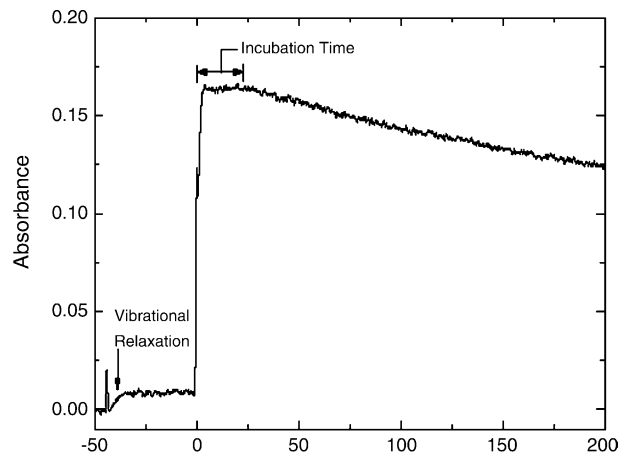


Fig. 2. Example CO_2 absorbance ($\ln(I_0/I)$) at $216.5\ \text{nm}$ for experiment with thermal decomposition. Initial mixture: $2\% \text{CO}_2/\text{Ar}$. Vibrationally equilibrated incident shock conditions: $1812\ \text{K}$ and $16.3\ \text{kPa}$. Initial (prior to decomposition) vibrationally equilibrated reflected shock conditions: $3838\ \text{K}$, $83.1\ \text{kPa}$. Note the vibrational relaxation after incident shock-heating and the incubation period prior to decomposition after reflected shock-heating.

the incident shock, it is not resolved after the reflected shock because the higher temperature and pressure behind the reflected wave have a much faster vibrational energy transfer rate. Following the passage of the reflected shock wave an incubation period is observed in the absorption prior to the thermal decomposition (Fig. 2). The reflected shock conditions are $3838\ \text{K}$ and $83.1\ \text{kPa}$ for the experiment in Fig. 2. This incubation period is somewhat longer than the vibrational relaxation time and is similar to behavior commonly seen in shock tube laser-schlieren experiments [21]. CO_2 has a large bond energy ($125.7\ \text{kcal/mol}$, $43970\ \text{cm}^{-1}$) and thus only the high-energy tail of the energy distribution plays a role in the dissociation, even at the high temperatures of this study. In the experiments reported here where the average thermal energy is significantly below the dissociation energy, thermal dissociation can only proceed when the highest vibrational levels are populated, and a steady dissociation rate is not established until the shock-heated CO_2 reaches a steady-state vibrational distribution in these high levels. The incubation period is longer than the vibrational relaxation time because the time required for vibrational relaxation in the low-lying vibrational levels is much shorter than the time required to reach the steady-state vibrational population in the highest levels. The incubation period is dependent on collisional transfer rates from the low-lying vibrational levels at the bottom of the energy ladder to the levels near the dissociation threshold [22]. It should be noted that the absorption cross-section was determined for these experiments in the incubation plateau prior to dissociation, and therefore, the cross-section determination does not

depend on knowledge of the subsequent chemistry. Additionally, the experimental temperature during the plateau is not in question for these high-temperature experiments because the CO₂ vibrational temperature equilibrates to the translational temperature within $\sim 1 \mu\text{s}$ (the vibrational relaxation time in these high-temperature decomposition experiments). To our knowledge this is the first observation of incubation prior to dissociation in CO₂. We plan to comprehensively examine this phenomenon in future work.

3. Results and discussion

The measured absorption cross-sections at the four wavelengths are plotted versus temperature in Fig. 3 and compared with the data from the earlier study from our laboratory [6]. We find excellent agreement for temperatures between 1800 and 2800 K; at higher temperatures, the extrapolation from the earlier lower temperature data would predict too large a cross section.

Due to the spectrally smooth nature of the UV CO₂ absorption feature [6] the current absorption cross-section results in Fig. 3 can be fit to a semi-empirical form $\ln \sigma(\lambda, T) = a + b\lambda$,

where $a = c_1 + c_2T + c_3/T$ and $b = d_1 + d_2T + d_3/T$. The cross-section, $\sigma(\lambda, T)$, is in units of $10^{-19} \text{ cm}^2 \text{ molecule}^{-1}$, the wavelength, λ , is in units of 100 nm, and the temperature, T , is given in units of 1000 K. The following parameters provide a best fit to the data: $c_1 = 0.05449$, $c_2 = 0.13766$, $c_3 = 23.529$, $d_1 = 1.991$, $d_2 = -0.17125$, and $d_3 = -14.694$. As is shown in Fig. 3 the scatter of

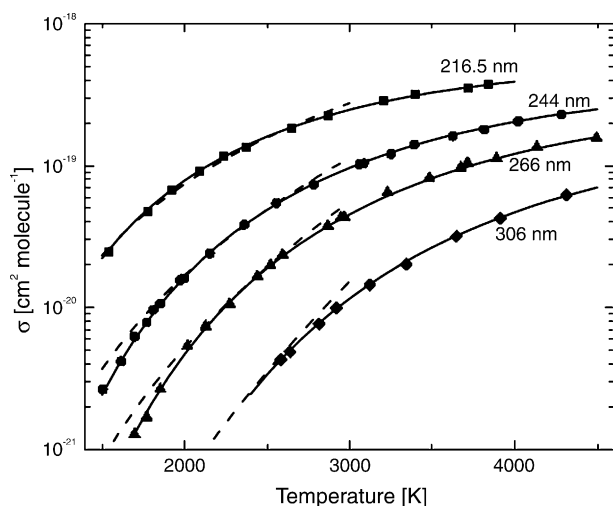


Fig. 3. Temperature-dependence of the UV CO₂ absorption cross-section. Solid symbols, experimental results: squares, 216.5 nm; circles, 244 nm; triangles, 266 nm; diamonds, 306 nm. Solid lines, semi-empirical fit to current data; dashed lines, Schulz et al. [6].

the data about the fit is quite small with a $1 - \sigma$ standard deviation of 1.8%. It should be noted that this semi-empirical expression for the absorption cross-section should not be extrapolated outside the temperature and wavelength range of the data, but based on experience from Schulz et al. [6] study interpolation is justified.

The absorption cross-section is plotted versus wavelength in Fig. 4 for selected temperatures below 3050 K to compare with Schulz et al. [6]; this comparison shows good agreement for temperatures below about 2800 K. The difference between the current measurement and the previous data at 3050 K can be attributed to over-estimation of the thermal decomposition in the earlier paper as discussed below.

The uncertainty in the CO₂ cross-sections obtained in these experiments is the result of uncertainties in the experimental temperature and pressure, uncertainties in the initial CO₂ concentration, and uncertainties associated with the signal-to-noise of a given experiment. The experiments in which the smallest absorption was monitored (low T and long λ) provide cross-sections with the highest uncertainty. The majority of the cross-section results have uncertainties less than 5%; only a few of the smallest absorption cross-sections measured at 244 and 266 nm have larger uncertainties, with the largest uncertainty of 14%.

A comparison of our new cross-section determinations with those of Schulz et al. [6] shows that the agreement is quite good in the middle of the temperature range, with deviations of 30% and 40%, respectively, at the highest and lowest temperatures of the Schulz et al. study which is within the reported uncertainty for those data at the low and high temperature extremes. At low temperatures the difference in our findings and Schulz

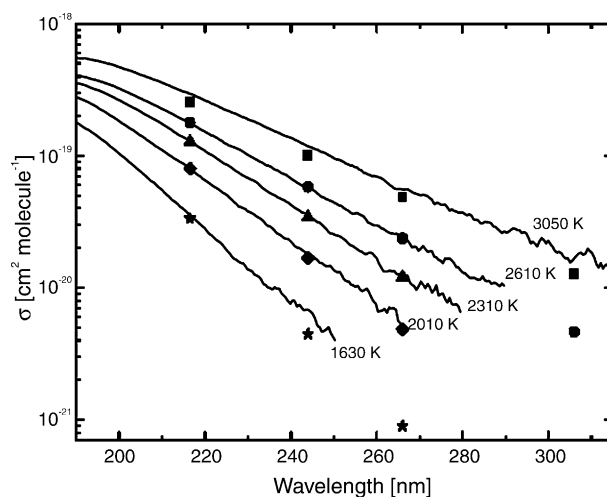


Fig. 4. Wavelength-dependence of the UV CO₂ absorption cross-section. Solid symbols, semi-empirical fit to current data: squares, 3050 K; circles, 2610 K, diamonds, 2010 K; stars, 1630 K. Solid lines, Schulz et al. [6].

et al. is likely due to limited signal-to-noise; as the noise in the spectra (Fig. 4) shows, the Schulz et al. results at low temperatures and long wavelengths are significantly more uncertain than the current results due to poorer signal-to-noise. At high temperatures our absorption cross-sections are lower than those of Schulz et al. due to their use of data impacted by CO₂ thermal decomposition. The current experiments indicate that the mechanism used in the Schulz et al. study (GRIMech 3.0) to account for decomposition by CO₂ has a rate coefficient for CO₂ → CO + O that is too fast. Schulz et al. calculated the average mole fraction of CO₂ during their averaging time period using the GRI mechanism, thus giving a low CO₂ mole fraction. Thus they inferred an absorption cross-section that is too large. We plan to re-evaluate the thermal decomposition of CO₂ in the future.

The hot CO₂ pre-dissociative absorption is a continuum spectral feature caused by the intersection of many electronic-vibrational-rotational lines, with a dense energy spectrum typical of a triatomic. If one uses a quasi-diatomic approximation to describe these optical transitions [23], it can be shown that the absorbance at a given wavelength, λ , is described by

$$\sigma(\lambda, T)n = \sigma_{\text{eff}}(\lambda)n_1 = [\sigma_{\text{eff}}(\lambda)n/Q_{\text{vib}}] \exp(-\varepsilon_1(\lambda)/kT),$$

where the average absorption takes place from a population with density n_1 at a lower state vibrational energy $\varepsilon_1(\lambda)$ above the zero-energy ground state and where $\sigma_{\text{eff}}(\lambda)$ is an effective cross-section for absorption. The vibrational partition function, Q_{vib} , is given by

$$Q_{\text{vib}} = [1 - \exp(-\theta_1/T)]^{-1} [1 - \exp(-\theta_2/T)]^{-2} \\ \times [1 - \exp(-\theta_3/T)]^{-1},$$

where $\theta_1 = 1999$ K, $\theta_2 = 960$ K, and $\theta_3 = 3383$ K. This description of the temperature-dependent absorption cross-section allows estimation of the effective vibrational energy of the absorbing lower state, $\varepsilon_1(\lambda)$. Fig. 5(a) shows a plot of the product of the measured cross-section, $\sigma(\lambda, T)$, with the vibrational partition function, Q_{vib} versus inverse temperature. This plot shows the product, $\sigma(\lambda, T)Q_{\text{vib}}$, is linear with a slope that provides an estimate of the absorbing lower state energy, ε_1 . The cross-section measurements provide lower state energies of 1.09 eV (8790 cm⁻¹), 1.48 eV (11940 cm⁻¹), 1.79 eV (14440 cm⁻¹), and 2.34 eV (18870 cm⁻¹) for absorption of photons at 216.5, 244, 266, and 306 nm, respectively; these results can be expressed with

$$\varepsilon_1(\lambda) = -1.94 + 0.014[1/\text{nm}]\lambda \text{ eV}.$$

The lower state energy results are compared to previous determinations made by Eremin et al. [24] (193 nm) and Zabelinskii et al. [25] (238 and 300 nm) in Fig. 5(b) with good agreement. Unfortunately, this simplified photophysical model does not allow for an assignment of the absorption at a given wavelength to a specific vibrational level(s) because of the complex nature of

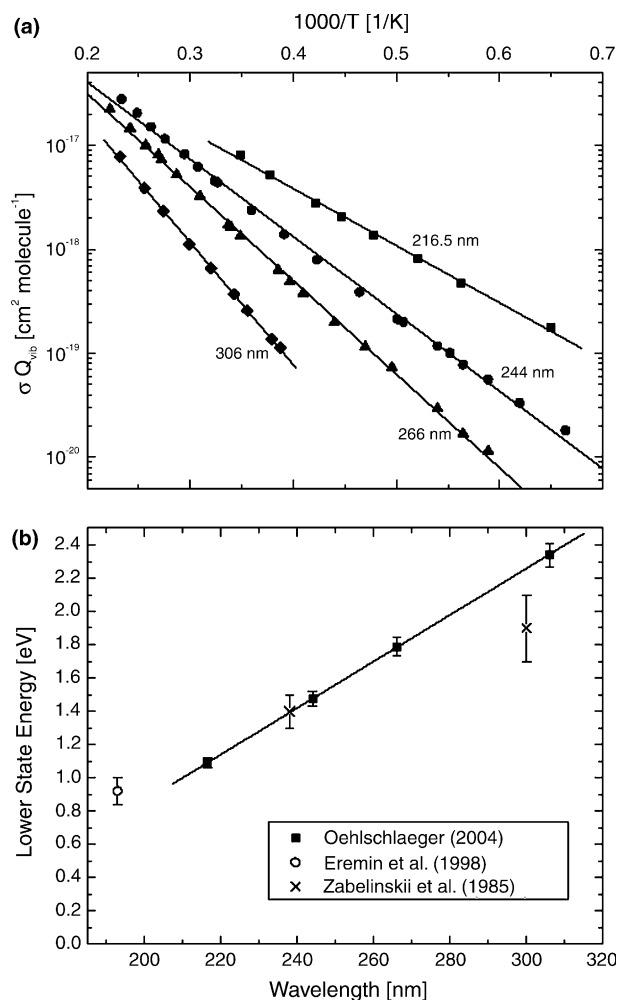


Fig. 5. Product of cross-section and vibrational partition function (σQ_{vib}) versus inverse temperature (a) and ground state energy versus wavelength (b). (a) Solid squares, 216.5 nm data; solid circles, 244 nm data; solid triangles, 266 nm data; solid diamonds, 306 nm data; solid lines, least-squares fit of form $\sigma(\lambda, T)Q_{\text{vib}} = \sigma_{\text{eff}}(\lambda)\exp(-\varepsilon_1/T)$. (b) Squares, current results; line, linear fit to current results; open circles, Eremin et al. [24]; \times , Zabelinskii et al. [25].

the triatomic energy spectrum. Also, note that the linearity of $\sigma(\lambda, T)Q_{\text{vib}}$ deviates slightly at the highest temperatures (Fig. 5(a)). This deviation might be caused by enhanced absorption due to transitions to electronic states other than ¹B₂ such as ¹A₂, ³A₂, and ³B₂ that occurs at the highest temperatures where there is more highly excited population.

The improved determinations of the CO₂ absorption cross-section presented here should enable absorption-based thermometry in the high-temperature post-combustion gases in a variety of practical systems. For example, a two-wavelength temperature sensor using 244 and 266 nm laser radiation in a combustion system with 10% CO₂ at 1 atm, a 10 cm path length, and an uncertainty in absorbance of 0.1% ($\ln(I_0/I) = 0.001$), could be used to measure temperature over the range of 1900–4500 K with an uncertainty of 6% at 1900 K

and 2% at 4500 K. Note, these two wavelengths are longer than the primary absorption due to aliphatic hydrocarbons, NO, and O₂, and shorter than the OH absorption feature at 306 nm, and thus avoid interference from the major components of combustion effluent. Such a diagnostic scheme has excellent potential for high-temperature gases, especially at high-pressures such as those found behind detonation waves; this is a regime where many other schemes fail.

4. Conclusions

The absorption cross-section of shock-heated carbon dioxide has been measured at four different laser wavelengths (216.5, 244, 266, and 306 nm) in the temperature range of 1500–4500 K. The high spectral brightness provided high signal-to-noise ratios and microsecond time resolution, which allowed accurate measurement of the absorption cross-section without the use of a chemical model to describe the decomposition of CO₂. These experiments show an incubation period prior to dissociation, observed for the first time in CO₂. The temperature dependence of the CO₂ cross-section was used to estimate the energy levels of the absorbing ground state. It was found that those molecules absorbing at 216.5, 244, 266, and 306 nm have characteristic vibrational energies of 1.09, 1.48, 1.79, and 2.34 eV, respectively.

Acknowledgements

This work has been supported by the US Air Force Office of Scientific Research, Aerospace Sciences Directorate, with Julian Tishkoff as the technical monitor. The authors thank David Rothamer (Stanford) for discussions regarding vibrational energy transfer in CO₂.

References

- [1] H. Okabe, *The Photochemistry of Small Molecules*, Wiley, New York, 1978.
- [2] M. Koshi, M. Yoshimura, H. Matsui, *Chem. Phys. Lett.* 176 (1991) 519.
- [3] R.J. Jensen, R.D. Guettler, J.L. Lyman, *Chem. Phys. Lett.* 277 (1997) 356.
- [4] M. Ogawa, *J. Chem. Phys.* 54 (1971) 2550.
- [5] B.R. Lewis, J.H. Carver, *J. Quant. Spectrosc. Radiat. Transfer* 30 (1983) 297.
- [6] C. Schulz, J.D. Koch, D.F. Davidson, J.B. Jeffries, R.K. Hanson, *Chem. Phys. Lett.* 355 (2002) 82.
- [7] J.B. Jeffries, C. Schulz, D.W. Mattison, M.A. Oehlschlaeger, W.G. Bessler, T. Lee, D.F. Davidson, R.K. Hanson, *Proc. Combust. Inst.* 30 (2004) 1545.
- [8] N.A. Generalov, S.A. Losev, V.A. Maksimenko, *Dokl. Akad. Nauk. SSSR* 150 (1963) 839.
- [9] M. Ibreighith, P. Roth, *Forsch. Ing.-Wes.* 46 (1980) 173.
- [10] K.T. Hartinger, S. Nord, P.B. Monkhouse, *Appl. Phys. B* 70 (2000) 133.
- [11] T. Joutsenoja, A. D'Anna, A. D'Alessio, M.I. Nazzaro, *Appl. Spectrosc.* 55 (2001) 130.
- [12] T. Lee, W.G. Bessler, C. Schulz, M. Patel, J.B. Jeffries, R.K. Hanson, *Appl. Phys. B* 79 (2004) 427.
- [13] W.G. Bessler, C. Schulz, T. Lee, J.B. Jeffries, R.K. Hanson, *Chem. Phys. Lett.* 375 (2003) 344.
- [14] D.W. Mattison, M.A. Oehlschlaeger, C.I. Morris, Z.C. Owens, E.A. Barbour, J.B. Jeffries, R.K. Hanson, *Proc. Combust. Inst.* 30 (2004) 2578.
- [15] M.A. Oehlschlaeger, D.F. Davidson, R.K. Hanson, *J. Phys. Chem. A* 108 (2004) 4247.
- [16] J.T. Herbon, Ph.D. Thesis, Stanford University, Stanford, CA (2004).
- [17] J.T. Herbon, R.K. Hanson, D.M. Golden, C.T. Bowman, *Proc. Combust. Inst.* 29 (2002) 1201.
- [18] C.J.S.M. Simpson, T.R.D. Chandler, A.C. Strawson, *J. Chem. Phys.* 51 (1969) 2214.
- [19] G. Kamimoto, H. Matsui, *J. Chem. Phys.* 53 (1970) 3990.
- [20] A. Spielfiedel, N. Feautrier, C. Cossart-Magos, G. Chambaud, P. Rosmus, H.J. Werner, P. Botschwina, *J. Chem. Phys.* 97 (1992) 8382.
- [21] J.H. Kiefer, S.S. Kumaran, S. Sundaram, *J. Chem. Phys.* 99 (1993) 3531.
- [22] J.E. Dove, *J. Troe, Chem. Phys.* 35 (1978) 1.
- [23] A.V. Eremin, V.S. Ziborov, V.V. Shumova, P. Roth, *Chem. Phys. Rep. (Transl. Khim. Fiz.)* 17 (1988) 1275.
- [24] A.V. Eremin, V.S. Ziborov, I.M. Naboko, *Sov. Opt. Spektrosk.* 67 (1989) 562.
- [25] I.E. Zabelinskii, I.S. Zaslanko, L.B. Ibragimova, Y.K. Mukoseev, S.V. Slinkin, O.P. Shatoalov, *Zh. Prik. Spektrosk.* 4 (1985) 1466.